

# Experimental and calculated phase equilibria in the cubic BN–Ta–C system

E. Benko<sup>a,b,\*</sup>, T.L. Barr<sup>c</sup>, A. Bernasik<sup>c</sup>, S. Hardcastle<sup>c</sup>, E. Hoppe<sup>c</sup>,  
E. Bielańska<sup>d,e</sup>, P. Klimczyk<sup>a</sup>

<sup>a</sup>*Institute of Metal Cutting, 37A Wroclawska Str., 30-011 Kraków, Poland*

<sup>b</sup>*University of Bielsko-Biała, Willowa 2Str., 43-309 Bielsko-Biała, Poland*

<sup>c</sup>*Materials Department and Laboratory for Surface Studies, University of Wisconsin-Milwaukee, Milwaukee, WI 53201, USA*

<sup>d</sup>*Surface Spectroscopy Laboratory, University of Mining and Metallurgy, 23 Reymonta Str. 30-059 Kraków, Poland*

<sup>e</sup>*Institute of Metallurgy and Materials Science, 25 Reymonta Str., 32-050 Kraków, Poland*

Received 22 July 2002; received in revised form 31 January 2003; accepted 3 March 2003

## Abstract

Theoretical and experimental studies of cubic BN mixed with Ta and TaC in the 1:1 molar ratio are presented. From theoretical calculations it follows that Ta reacts with boron nitride forming additionally two phases: tantalum boride and tantalum nitride. Experimental cBN-phase composites were prepared by high pressure hot pressing. The samples were characterized after heat treatment using scanning electron microscopy (SEM), X-ray diffraction (XRD) and X-ray photoelectron spectroscopy (XPS).

© 2003 Elsevier Ltd and Techna S.r.l. All rights reserved.

**Keywords:** A. Hot pressing; B. Composites; B. Spectroscopy; Solid state reaction

## 1. Introduction

Cubic boron nitride has high hardness, high heat conductivity and high electric insulating properties, second only to diamond and moreover, has better chemical stability and resistance to oxidation, with better heat and thermal shock resistance than diamond. While diamond has a high affinity with iron group metals, cubic boron nitride has a low affinity with them [1–5].

Cubic boron nitride (cBN) sintered compacts have a wide range of potential applications in cutting tools, structural materials and as heat sinks because of their good thermal conductivity and hardness. There are several kinds of binders for cBN compacts because cutting conditions are affected by workpiece materials, cutting methods, etc.

In order to obtain composite materials with these optimal properties, it is important to elucidate whether any chemical reactions occur at nitride/carbide or metal

interfaces, for example, those involving BN–Ta/TaC composites.

Ceramics like TiC, TaC and sometimes metals like Ti, Ta, Co are commonly used for binders [6,7]. In this paper, we present the results of the investigations of cBN–Ta and cBN–TaC composite materials. A systematic study of their phase equilibria and structural chemistry is presented.

## 2. Chemical equilibria in the BN–Ta/TaC systems

Calculations of phase equilibria for the BN–Ta/TaC system were carried out using the VCS algorithms. The abbreviation originates from the first letters of its authors: Villars, Cruise and Smith [8,9]. This algorithm belongs to a group of the so-called stoichiometric algorithms, i.e. stoichiometric coefficients of chemical reactions by which the system reaches the equilibrium state are taken into account. The algorithm requires that its user merely lists chemical compounds that can co-exist in the equilibrium state together with their standard thermochemical potentials of formation; knowledge of

\* Corresponding author. Tel.: +48-12-631-7330; fax: +48-12-633-9490.

E-mail addresses: ewa.benko@ios.krakow.pl (E. Benko).

the number and types of independent reactions is not necessary for the calculations.

The algorithm is based on minimization of the thermodynamical potential of the whole reacting mixture [Eq. (1)] and this potential is expressed by reaction-extent variables related to the number of moles by Eq. (2).

$$g = \sum_{i=1}^N n_i \cdot \mu_i = (\min) \quad (1)$$

$g$ —thermodynamical potential of the whole reacting system;  $n_i$ —number of moles of the  $i$  component;  $\mu_i$ —chemical potential of the  $i$  component; and  $N$ —number of components, where:

$$n_i = n_i^o + \sum_j^R \gamma_{ij} \cdot \xi_j \quad i = 1, 2, \dots, N' \quad (2)$$

$n_i^o$ —starting number of moles of the  $i$  component;  $\mu_{ij}$  stoichiometric coefficient of the  $i$  component in  $j$ —reaction;  $\xi_j$ —reaction-extent variable of  $j$  reaction;  $R$ —number of independent reactions; and  $N'$ —number of components without the inert ones.

Thus in the VCS algorithm the non-linear function of many variables  $f(x)$  is minimized:

$$f(x) = \min$$

where  $x$ —a vector of many variables.

The equilibria compositions in the following systems have been calculated: BN–Ta, and BN–TaC systems for the molar ratios of BN:metal equal to 1:1 over a wide range of pressure ( $1.3 \times 10^{-3}$ – $1 \times 10^8$  Pa) and temperature (27–2427 °C). The data necessary for the calculations (e.g. standard thermodynamical potentials of formation) have been taken from the appropriate reference data [11,12].

It has been found from the calculations that all the phases mentioned above react with boron nitride forming new phases.

### 2.1. BN–Ta system

The following components have been taken into account in the chemical equilibria calculations in this systems:  $N_2(g)$ ,  $B(g)$ ,  $B_2(g)$ ,  $BN(g)$ ,  $Ta(g)$ ,  $B(l)$ ,  $TaB_2(s)$ ,  $Ta_2N(s)$ ,  $B(s)$ ,  $TaN(s)$ ,  $Ta(s)$ ,  $BN(s)$  where  $g$ ,  $l$  and  $s$  refer to gas, liquid or solid, respectively.

Calculations have been carried out in the temperature range of 27–2127 °C and pressure range  $1.3 \times 10^{-3}$ – $1 \times 10^8$  Pa. For the molar ratio BN:Ta equal to 1:1 and independent of temperature, three solid phases co-exist: BN (0.33 mol),  $TaB_2$  (0.33 mol) and TaN (0.67 mol). Starting from 927 °C under low pressure, nitrogen appears in the system (0.25 mol), BN disappears, and

$TaB_2$  and TaN (0.5 mol each) are the only solid phases present. The pressure range in which these phases exist expands as the temperature increases from  $1.3 \times 10^{-3}$  Pa for 923 °C to 3 Pa for 1223 °C. Under higher pressures the chemical equilibria states are exactly the same as in the temperature range 27–827 °C. At 1327 °C and extremely low pressures,  $Ta_2N$  in the amount of 0.25 mol appears in the system whereas TaN disappears. As the temperature increases the temperature range in which  $Ta_2N$  and  $TaB_2$  co-exist shifts to higher pressure values. Thus for 1323 °C the critical pressure equals  $1.3 \times 10^{-3}$  Pa and for 2227 °C it is  $3 \times 10^1$  Pa– $1 \times 10^2$  Pa. Starting from 1523 °C gaseous boron appears, whereas at 1623 °C tantalum (solid) in the amount of 0.5 mol exists with  $TaB_2$  (0.49 mol). The pressure range in which these phases exists widens; at 1827 °C it reaches  $7 \times 10^{-1}$  Pa. At 1927 °C gaseous tantalum appears in the system. Starting from this temperature up to 2127 °C under extremely low pressure only gaseous  $N_2$ , B and Ta as well as solid Ta exist in the system. The pressure range in which only solid phases,  $TaB_2$  and TaN, are present shifts to higher pressure values from  $1.3 \times 10^{-3}$  Pa for 927 °C to  $2 \times 10^{-2}$ – $2 \times 10^5$  Pa at 2127 °C. Similarly the pressure range of coexistence of BN (0.33 mol),  $TaB_2$  (0.33 mol) and TaN (0.67 mole) changes from  $5 \times 10^{-3}$ – $1 \times 10^8$  Pa for 927 °C to  $3 \times 10^5$ – $1 \times 10^8$  Pa for 2127 °C. For the BN:Ta molar ratio equal to 2:1, chemical equilibria are similar to the ones calculated for the 1:1 molar ratio. In the range 27–827 °C, three solid phases exist namely: BN (1.33 mol),  $TaB_2$  (0.33 mol) and TaN (0.67 mol). Starting from 927 °C and at low pressure, only one solid phase exists in the system, i.e.  $TaB_2$  (1 mol) besides gaseous  $N_2$  (1 mol). As the temperature increases the pressure range in which only one solid phase is present ( $TaB_2$ ) shifts to higher pressure values until at 2127 °C it is equal to  $3 \times 10^{-2}$ – $2 \times 10^5$  Pa. Graphical representation of chemical equilibria for this system for the temperature of 1400 °C is shown in Fig. 1.

### 2.2. BN–TaC system

The following components have been taken into account in the chemical equilibria calculations in this system:  $N_2(g)$ ,  $B(g)$ ,  $B_2(g)$ ,  $BN(g)$ ,  $Ta(g)$ ,  $C(g)$ ,  $CB(g)$ ,  $CN(g)$ ,  $CN_2(g)$ ,  $NCN(g)$ ,  $C_2(g)$ ,  $C_2N(g)$ ,  $C_2N_2(g)$ ,  $C_3(g)$ ,  $C_4(g)$ ,  $C_4N_2(g)$ ,  $C_5(g)$ ,  $B(l)$ ,  $CB_4(l)$ ,  $TaB_2(s)$ ,  $Ta_2N(s)$ ,  $B(s)$ ,  $TaN(s)$ ,  $Ta(s)$ ,  $BN(s)$ ,  $TaC(s)$ ,  $Ta_2C(s)$ ,  $C(s)$ ,  $CB_4(s)$ . The calculations have been carried out for temperature and pressure ranges 27–2400 °C and  $1.3 \times 10^{-3}$ – $1 \times 10^8$  Pa. In the system considered no chemical reactions occur up to 1127 °C at either for the BN:Ta molar ratio 1:1 or 2:1. At this temperature and under low pressure, a new solid phase appears at the BN:Ta molar ratio equal to 1:1, namely  $TaB_2$ , in the amount of 0.5 mol; nitrogen and solid carbon also occur. As

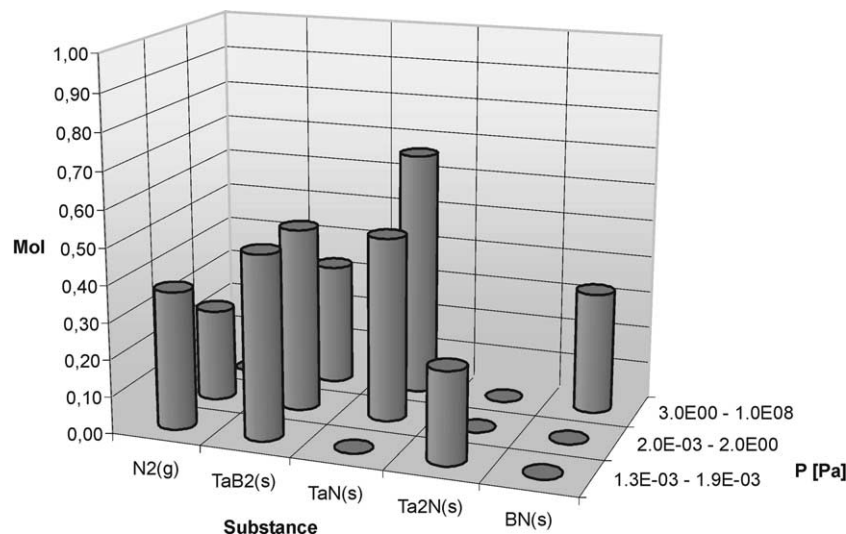


Fig. 1. Chemical equilibria in the BN:Ta = 1:1 system at the temperature of 1400 °C.

the temperature increases the pressure range in which  $\text{TaB}_2$  is present widens until at 2400 °C it reaches  $1 \times 10^4$  Pa. With increasing temperature gaseous B, C,  $\text{C}_3$ , CN, BN,  $\text{C}_2$ ,  $\text{C}_2\text{N}$ , CB appear. At the BN:TaC molar ratio equal to 2:1 a new solid phase,  $\text{TaB}_2$ , appears above 1127 °C at a pressure of  $1.3 \times 10^{-3}$  Pa. On the other hand, there exist pressure and temperature ranges for which this phase is the only thermodynamically stable one, except for C and  $\text{N}_2$ . With increasing temperature the pressure range in which  $\text{TaB}_2$  phase is present becomes wider and at 2127 °C it reaches  $1 \times 10^{-4}$  Pa. Pressure and temperature ranges in which the gaseous phases appear in the system are similar to the system of BN:TaC molar ratio equal to 1:1. Typical graphical representations of chemical equilibria in this system at 1400 °C are shown in Fig. 2.

### 3. Experimental procedure

#### 3.1. Substrate materials

Two types of BN/Ta/TaC samples were prepared, namely powdered and layered samples.

Powdered samples in the form of the 1:1 molar ratio mixture of boron nitride (ABN-300, De Beers, 3–5  $\mu\text{m}$  size) and tantalum/tantalum carbide (HC Starck, 3–5  $\mu\text{m}$  size) were mechanically mixed in ethyl alcohol. The mixed powder was pressed into a disc 15 mm in diameter and 4 mm in height. The whole reaction input which—besides a graphite heater—contained several pyrophyllite elements as well as molybdenum contact plates (Fig. 3) were sintered in a high pressure press PH0044 equipped with a Bridgman cavity chamber. The samples were

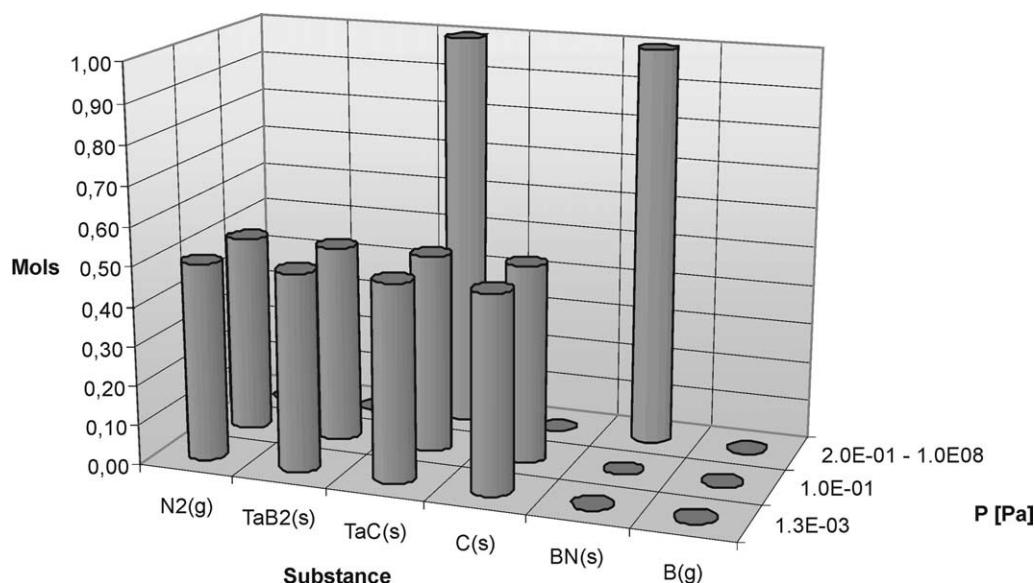


Fig. 2. Chemical equilibria in the BN:TaC = 1:1 system at the temperature of 1400 °C.

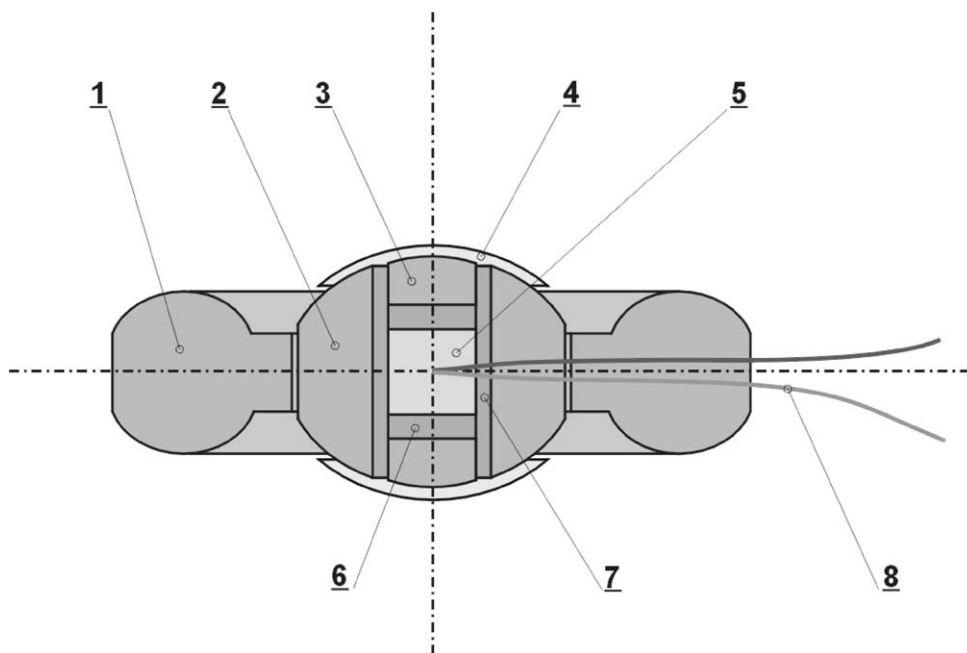


Fig. 3. Reaction input for sintering cBN composites: 1, 2, calcite sleeve 3, pyrophyllite shields; 4, molybdenum shields; 5, sintered composite; 6, 7, graphite heater; 8, thermoelement.

sintered at 7 GPa, 1750 °C for 3.5 min: the pressed compact was subsequently polished and its microstructure and mechanical properties examined. After this the samples were heat-treated in vacuum at 1400 °C for 2 h.

The layered Ta/TaC+cBN samples were prepared using the PVD magnetron sputtering method and the layered samples subsequently heated in vacuum at 1600 °C for 2 h.

The cBN plates were obtained during direct transformation of hexagonal boron nitride powder at 2800 °C and a pressure of 9 GPa. The chemical composition of cBN was found to be C—0.04, Ca—0.05, Si—0.02, Mg—0.002, Mg—0.004 at.%. The resulting disks were 6 mm in diameter and 1 mm high. The surface was polished using an abrasive grain size of 220  $\mu\text{m}$ . Prior to the deposition, BN substrates were cleaned ultrasonically in three steps using acetone, trichloroethylene and propyl alcohol for 15 min each. The TaC film was grown by the magnetron sputtering method: evaporation of pure Ta into argon and reactive 99.99%  $\text{CH}_4$  gas (TaC coating) at a chamber pressure  $1.5 \times 10^{-1}$  Pa for 5 min at 1.5 V. Thickness of the layer was 500 Å.

### 3.2. X-ray diffraction studies

Four types of samples were investigated:

1. Ta-foil.
2. Composite samples 1:1 BN:Ta ratio hot pressed ( $T=1750$  °C,  $P=7$  GPa) and thermally heated at 1400 °C, 2 h.
3. Composite samples 1:1 BN:TaC ratio hot pressed

( $T=1750$  °C,  $P=7$  GPa) and thermally heated at 1400 °C, 2 h.

4. Samples of cBN with TaC, layered by the magnetron sputtering method, thermally heated at 1600 °C, 2 h.

X-ray diffraction studies have been carried out using a Philips 1710 diffractometer equipped with  $\text{CuK}_\alpha$  radiation [13]. Identifications were done using an APD-3.5B computer program based on the selected diffraction data from the JCPDS.

### 3.3. SEM studies

The BN–TaC interface layer has been studied using scanning electron microscopy (Philips, type XL-30) equipped with a EDS-ISIS-Link detector.

### 3.4. TEM studies

Samples for microscopic studies were obtained from the sinters by ultrasonic treatment, preliminary mechanical polishing and then ion etching in a DuoMill apparatus produced by Gatan Company. Microstructure observations were carried out by transmission electron microscopy with a Philips EM 301 and Philips CM20 equipped with EDS set up for local phase analysis.

### 3.5. XPS studies

XPS studies were generally performed on a Hewlett-Packard (HP) 5950A, spectrometer with a high-resolution

X-ray monochromator, using an Al  $K_{\alpha}$  (1476 eV) anode at an irradiation power of 600 W. General calibration produced a binding energy scale specified by Au ( $4f_{7/2}$  =  $83.98 \pm 0.05$  at a line width of  $< 1.0$  eV. The charging shifts produced by the insulating samples were removed by a combination of electron flood gun adjustments and fixing the C1s binding energy of the hydrocarbon part of the adventitious carbon line at 284.6 eV [10].

Studies of the surface composition of Ta–BN and TaC–BN systems were preceded by the analysis of the spectra of Ta at various oxidation levels (Fig. 1). In these studies pure Ta foil coated with  $Ta_2O_5$  was used and examined by XPS; the foil surface was sputtered with an Ar<sup>+</sup> beam and analysed again using XPS (Fig. 2). The best spectrum fitting of the  $4f$  Ta peaks was obtained using three doublet lines ( $4f_{7/2}$  and  $4f_{5/2}$ ) of the spin-orbit splitting 1.85 eV and the line width 1.4 eV. Individual lines can be ascribed to: Ta atoms present in  $Ta_2O_5$  (Ta  $4f_{7/2}$  = 26.9 eV), partly reduced Ta–O (B.E. = 22.3 eV) and metallic Ta (B.E. = 21.3 eV). The results obtained are collected in Table 1.

The photoelectron peaks for Ta(2p), B(1s), O(1s), N(1s), C(1s) of the investigated samples (BN+TaC)

were examined in order to characterise the chemical interactions between BN and TaC.

The samples were also sputtered with 2.5 KeV argon ions to determine the chemical state of the substrate and interfacial features.

Curve fitting program of the data was performed after a Shirley background subtraction, using a two-point box curve fitting program with a Gaussian/Lorentzian product function.

## 4. Results and discussion

### 4.1. X-ray diffraction study

Representative diffraction pattern of BN:Ta/TaC 1:1 molar ratio composite heat treated at 1400 °C under  $1.3 \times 10^{-3}$  Pa (2 h) is presented in Fig. 4. In BN:Ta composites two additional phases, TaB and non-stoichiometric  $Ta_6N_{2.57}$ , are formed. These cannot be compared with calculated equilibrium composition because thermodynamical data for the nonstoichiometric compounds are not available. In BN–TaC composites one additional phase is formed, namely TaB. This has been confirmed by calculated equilibrium composition according to which only one binary phase, tantalum boride, should be formed (Fig. 5). In the cBN samples layered with TaC heat treated at 1600 °C under  $1.3 \times 10^{-3}$  Pa (2 h) there is also one additional phase formed, namely TaB. This has been confirmed by calculated equilibrium composition.

### 4.2. SEM investigations

The fracture of cBN sintered with Ta and TaC, Fig. 6, occurred by an intergrain mode; both look the same and are characteristic of this type of material. The surface fracture was very corrugated, running along separate

Table 1  
XPS data for Ta for foil surface

Sample	Ta°		Ta–O <sub>x</sub>		Ta <sub>2</sub> O <sub>5</sub>		O/Ta relative intensity of the elements
	<i>E<sub>B</sub></i> (eV)	Relative intensity	<i>E<sub>B</sub></i> (eV)	Relative intensity	<i>E<sub>B</sub></i> (eV)	Relative intensity	
Before sputtering	21.64	0.08	23.01	0.05	26.28	0.87	1.08
2 min– 2.5 KeV	21.01	0.07	22.28	0.07	25.96	0.86	0.70
+ 5 min– 4 KeV	21.32	0.37	22.90	0.21	25.94	0.42	0.69

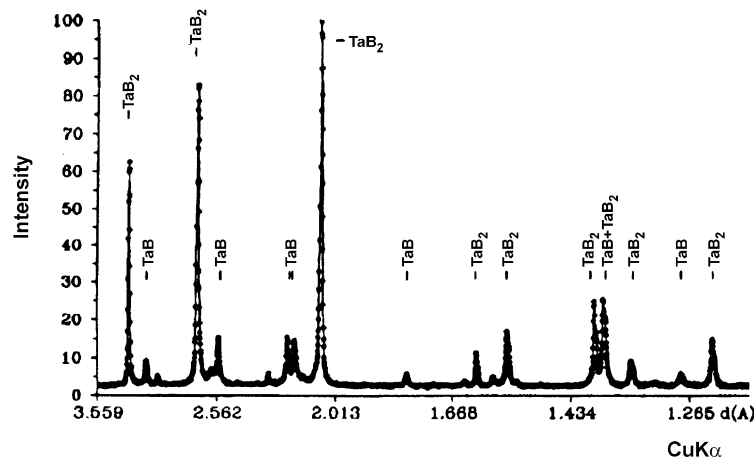


Fig. 4. XRD diffraction pattern from Ta/BN composite materials after heat treatment ( $T = 1400$  °C,  $P = 1.3 \times 10^{-3}$  Pa,  $t = 2$  h).



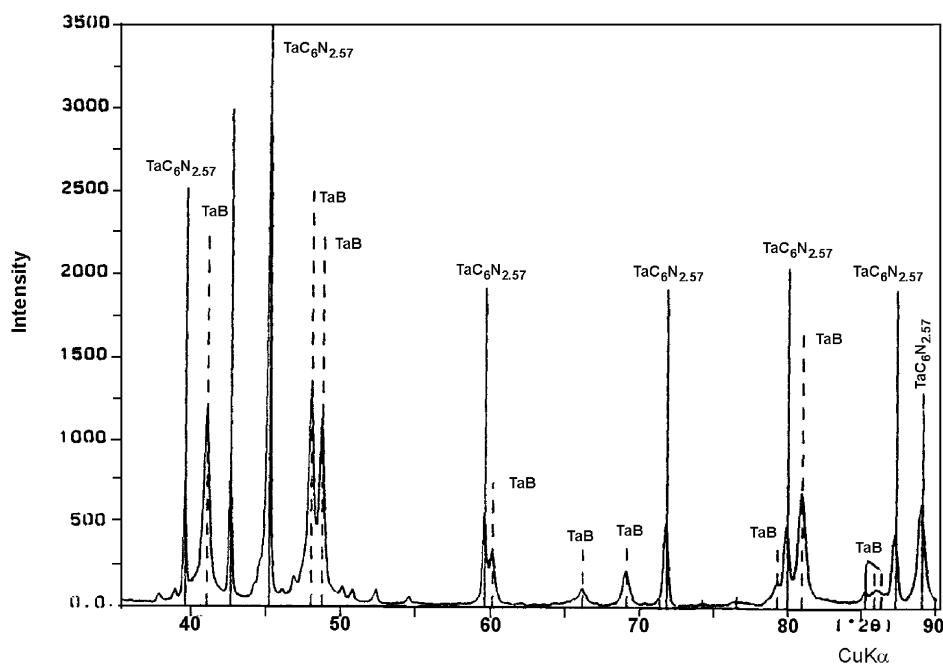


Fig. 5. XRD diffraction pattern from TaC/BN composite materials after heat treatment.

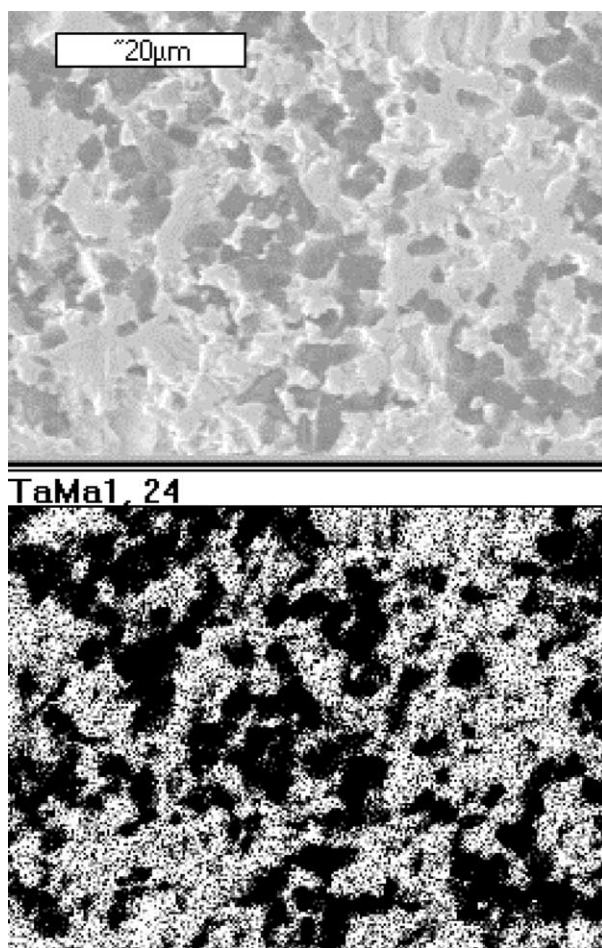


Fig. 6. Fracture surface of TaC/BN composite (a), and accompanying map of tantalum distribution (b).

BN grains boundaries with bright contrast at parts protruding from the BN–TaC. The darker areas resulted either from groves on the fractured surface or from the tantalum carbide added before sintering. The mapping, using the TaM $\alpha$  line and showing distribution of Ta in composite materials, is also presented in Fig. 6.

#### 4.3. TEM investigations

In the fine-crystalline areas of the cBN sintered with fine grained Ta in the boundary with BN and the coarser ones in the center of these areas were detected as in Fig. 7(a).

Elemental distribution mappings showed that in the center of fine-crystalline areas intensity of the signal corresponding to N increases which indicates that TaN appears in that spot [Fig. 7(b and d)]. In the areas occupied by fine crystallites of high density, characteristic flat defects appeared which were identified by electron diffraction as TaB and TaB<sub>2</sub> [Fig. 7(e,f)]. Boron distribution mapping [Fig. 7(c)] did not show any metal enrichment in that area because of the absorption of the B radiation by metal atoms or low collector efficiency for B, or both.

#### 4.4. XPS results

XPS was employed to investigate the chemical states of the BN–Ta and BN–TaC systems at 1400 and 1600 °C 2 h respectively and can be used to characterize the bonding and structure in above mentioned systems.

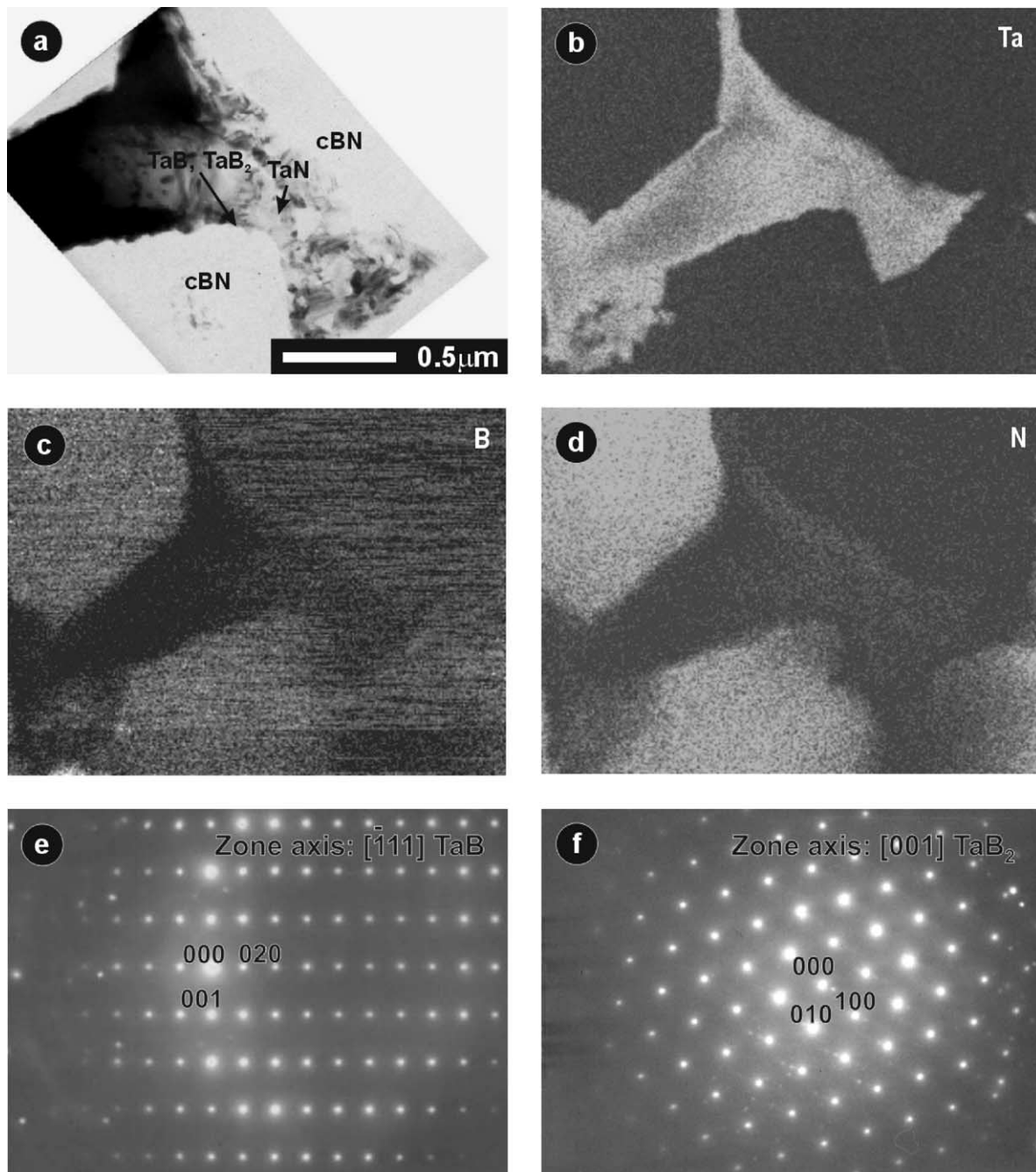


Fig. 7. Microstructure of cBN sintered with Ta (a) distribution mapping of Ta (b), B (c), N (d) and electron diffractions from the finely crystalline area in the boundary with BN (e, f).

XPS results for individual samples are collected in Tables 1–3. These tables give photoelectron binding energy values of the appropriate elements. Basing on these values individual chemical compounds present on the surface of the samples have been identified in accordance with literature data [10–12]. Relative intensities of the lines corresponding to the elements studied as well as the relative intensities of the lines due to various compounds of the same element are also collected. These values served as the basis for quantitative analysis of the samples.

An oxide layer was observed on the Ta foil surface, which was expressed by O/Ta relative intensity of 1.08 eV (Table 1, Fig. 8). After the first ion sputtering (2 min, 2.5 KeV) this relative intensity decreased to 0.70 but reduction of the tantalum signal was not observed. Relative intensities of Ta–elemental and Ta–O did not change. After the next sputtering (+ 5 min, 4 eV) (Fig. 9) an increase in the intensity of the peaks corresponding to reduced Ta was observed but O/Ta was not changed (Table 1). The sputtering process does not the

Table 2  
XPS data for Ta for all investigated samples

Sample	Ta <sup>o</sup>		Ta–O <sub>x</sub>		Ta <sub>2</sub> O <sub>5</sub>		O/Ta relative intensity of the elements	C/Ta relative intensity of the elements
	E <sub>B</sub> (eV)	Relative intensity	E <sub>B</sub> (eV)	Relative intensity	E <sub>B</sub> (eV)	Relative intensity		
TaC + BN (comp) 1400	21.94	0.38	23.13	0.05	25.39	0.57	3.62	1.84
Ta + BN (comp) 1400	22.07	0.34	23.81	0.09	25.74	0.57	2.39	0.32
Ta + BN (comp) 1400 after sputtering	22.05	0.36	24.12	0.11	26.30	0.53	0.78	0.27
Ta + BN layer 1600	E <sub>B</sub> 22.73 eV		Relative intensity 0.36		25.83	0.64	2.40	0.79

Table 3  
XPS data for B for all investigated samples

Sample	B–Ta		B–O		B/Ta relative intensity of the elements
	E <sub>B</sub> (eV)	Relative intensity	E <sub>B</sub> (eV)	Relative intensity	
TaC + BN (comp) 1400	187.65	0.19	190.75	0.81	0.24
Ta + BN (comp) 1400	187.25	0.46	190.76	0.54	0.11
Ta + BN (comp) 1400 after sputtering	187.07	0.34	191.75	0.66	0.11
Ta + BN layer 1600	187.90	0.55	191.82	0.45	0.16

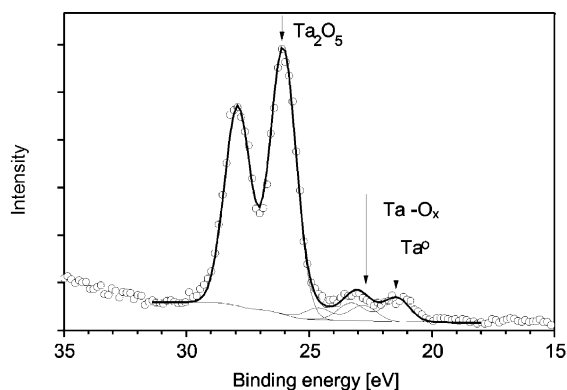


Fig. 8. Ta4f photoelectron spectrum of sample 1.

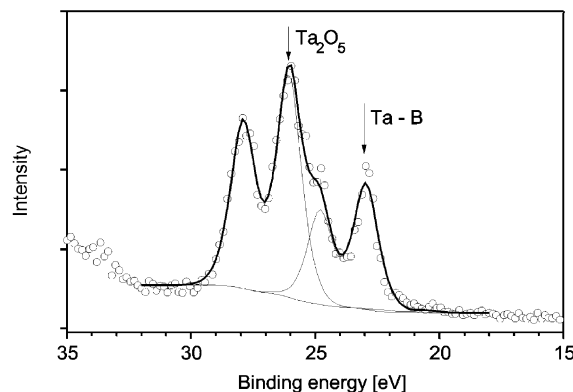


Fig. 10. Ta4f photoelectron spectrum of sample 4.

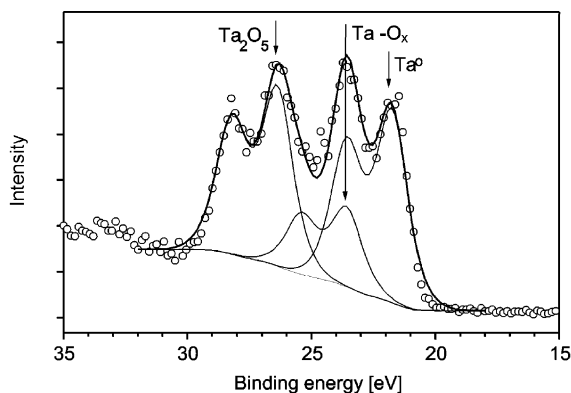


Fig. 9. Ta4f photoelectron spectrum of the sample 1 after sputtering.

clean surface of the samples from Ta oxide but reduces Ta<sub>2</sub>O<sub>5</sub> to Ta<sub>2</sub>O<sub>5-x</sub>.

It was observed that the surface O/Ta values were higher than on the Ta foil surface and ranged between 2.4 and 3.6. (Table 2) The highest value of the O/Ta value was observed for TaC–BN(1400 °C) (sample 3, Table 2, Fig. 12). As a result of ion sputtering a decrease in the O intensity was observed. The Ta–BN surface, heated at 1400 °C, decreased in its O/Ta value from 2.39 to 0.78 and only partly decreased contents of carbon was observed. Investigations of the cBN plates layered with Ta (Ta–BN, 1600 °C) showed altered surface composition (Table 2, Fig. 10): the peak corresponding to Ta–metal line was not observed and the Ta 4f spectrum showed two doublets: one corresponding to Ta<sub>2</sub>O<sub>5</sub> (which was present in the spectra of all the samples) and



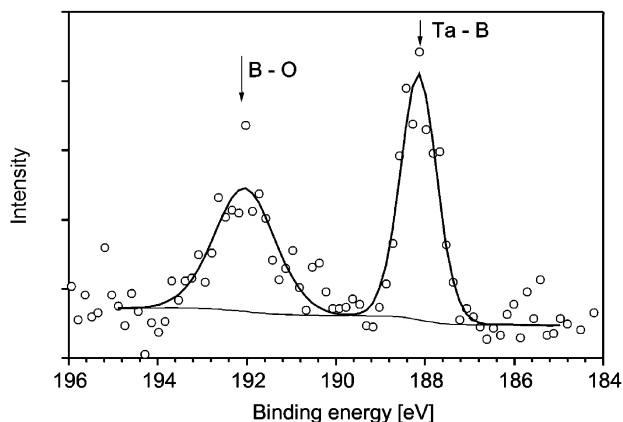


Fig. 11. B1s photoelectron spectrum of sample 4.

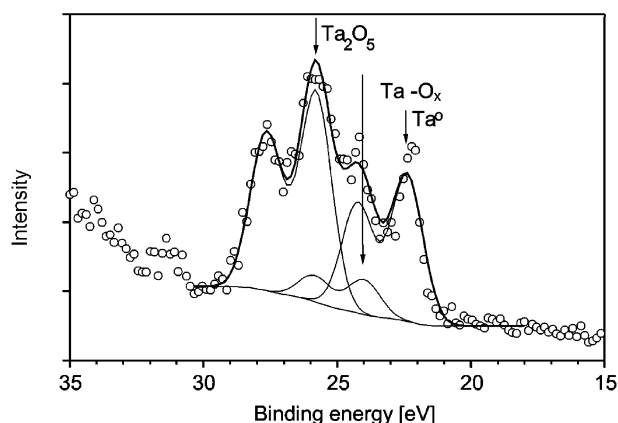


Fig. 12. Ta4f photoelectron spectrum of sample 3.

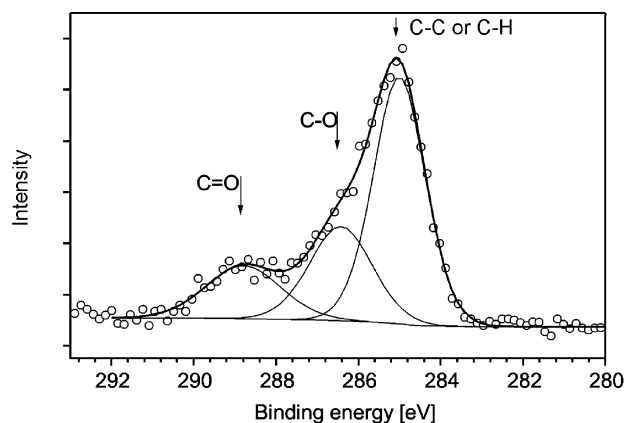


Fig. 13. C1s photoelectron spectrum of sample 3.

the second corresponding to the energy in the  $4f\ 7/2$  doublet between Ta-metal and TaO. This informs us about formation of a new phase.

As a result of B investigations the presence of two compounds was established. (Table 3). By analogy to Ti-B-N, B1s of the lowest energy can be ascribed to Ta-BN-1600 °C, which had the highest share of boron energy among all investigated samples (Figs. 10 and 11).

Hence, it can be concluded that the volume fraction of the new phase (TaB) is greatest in the layered TaC-BN sample.

The highest C:Ta ratio was observed on TaC-BN composite surface (Table 2, Fig. 13). Nitrogen 1s was not observed in all samples. The absence of nitrogen in the Ta + BN composite sample heat-treated at 1400 °C is due to polishing the sample before heat treatment; this resulted in the removal of some Ta from the surface since Ta is a softer phase than BN. Therefore after polishing the BN:Ta molar ratio at the surface is equal to 2:1. According to calculations only tantalum boride is formed as a new phase in this system.

## 5. Conclusions

XRD revealed the presence of crystalline TaB and nonstoichiometric  $Ta_6N_{2.57}$  phases in the Ta-BN system and one additional phase TaB in the TaC-BN system. In BN:Ta composites formation of two phases cannot be compared with calculated equilibrium composition because thermodynamic data for the non-stoichiometric compounds are not available. Formation of additionally phases in the BN-TaC composites has been confirmed by calculated equilibrium composition according to which only one binary phase, tantalum boride, should be formed (Fig. 5). The microstructure of cBN sintered with Ta/TaC is dense and the binding phase is uniformly distributed in its volume. TEM observation exhibited a system showing the formation TaB,  $TaB_2$  and TaN at the BN/Ta interface.

It was observed by XPS that on the surface of all samples formation of  $Ta_2O_5$ . XPS analysis of 1400 and 1600 °C treated Ta + BN and TaC + BN showed no TaN on the surface all samples. XPS data of sputtered Ta-foil and Ta-BN samples decrease of the O/Ta value was observed. XRD study shows that two phases, i.e. borides and nitrides of tantalum are formed in the Ta/BN composite samples. After XPS investigations only one new phase—tantalum boride—is visible. This information is very interesting from the technological point of view, because the phase content at the composites surface exerts a strong influence on their mechanical parameters. Formation of tantalum boride on the surface of the composite materials is not desirable from applicational point of view because of brittleness of the boride phase. Therefore this phase should be removed, e.g. by grinding.

## Acknowledgements

This study is based on the work sponsored by the Polish State Committee for Scientific Research (Grant No. 7 T08D 014 17).

## References

- [1] R.A. Anderson, CBN composites, *Adv. Mater. Proc.* (1989) 3.
- [2] H. Fuji, New composites material, in: *Int. Conference on Advanced Composites Mater*, Japan, 1993.
- [3] A.M. Mazurenko, et al., *Technologičeskie osobennosti primienija plastin STM v režuščem instrumene*, *Stanki i instrument* (1984) 7.
- [4] W.P. Modenov, et al., *Novyj sverchtverdyj kompozicionnyj material*, *Almazy i sverchtverdyje mater.* (1982) 10.
- [5] J.V. Najdič, et al., *Brazing and Metallization of Superhard Tool Materials*, Kiev, 1977.
- [6] N.J. Pipkin, et al., *Amborite—a remarkable new material*, *De Beers, Ind Diamond Rev.*, 1980.
- [7] J. Franzen, New generation of PCBN inserts boosts productivity in hard part turning, in: *An International Technical Conference on Diamond, Cubic Boron Nitride and Their Applications*, Vancouver, Canada, 2000.
- [8] W.P. Smith, R.W. Missen, *Chemical Reaction Equilibrium Analysis: Theory and Algorithms*, John Wiley & Sons, New York, 1982.
- [9] D.R. Stull, M. Prophet, *JANAF Thermochemical Tables*, second ed., National Bureau of Standards, NSRDS-NBS37, Washington, DC, 1971.
- [10] T.L. Barr, *Modern ESCA*, CRC, Boca Raton, FL, 1994.
- [11] D. Wagner, D.M. Bickham, *NIST X-ray Photoelectron Spectroscopy Database*; National Institute of Standards and Technology, Gaithersburg, MD 20899, October 1989.
- [12] T.L. Barr, S. Seal, *J. Vac. Sci. Technol. A* 13 (1995) 1239.
- [13] L. Mirkin, *I Spravocnik po rentgenostrukturnomu analizu polikristallow*, Moskwa, 1961.